

# Effect of orodispersible hyaluronic acid film on palatal mucosa wound healing

Jeong Hyun Lee<sup>1</sup> | Ko Eun Lee<sup>2</sup>  | Sang Wook Kang<sup>3</sup>  | Seung Hwan Park<sup>1</sup>  |  
 Yong Kwon Chae<sup>1,2</sup>  | Myoung-Han Lee<sup>4</sup> | Dong-Keun Kweon<sup>4</sup> | Sung Chul Choi<sup>2,5</sup>  |  
 Ok Hyung Nam<sup>2,5</sup> 

<sup>1</sup>Department of Dentistry, Graduate School, Kyung Hee University, Seoul, South Korea

<sup>2</sup>Department of Pediatric Dentistry, Kyung Hee University College of Dentistry, Kyung Hee University Medical Center, Seoul, South Korea

<sup>3</sup>Department of Oral and Maxillofacial Pathology, School of Dentistry, Kyung Hee University, Seoul, South Korea

<sup>4</sup>Jinwoo Bio Co. Ltd., Yongin-si, South Korea

<sup>5</sup>Department of Pediatric Dentistry, School of Dentistry, Kyung Hee University, Seoul, South Korea

## Correspondence

Ok Hyung Nam, Department of Pediatric Dentistry, School of Dentistry, Kyung Hee University, Kyungheedaero 26, Dongdaemoon-Gu, Seoul 02447, South Korea.

Email: [pedokhyung@gmail.com](mailto:pedokhyung@gmail.com)

## Funding information

Nano-Material Technology Development Program, Grant/Award Number: K210307002; National Research Foundation of Korea, Grant/Award Number: 2020R1C1C1006937; Supporting Project to evaluation New Domestic Medical Devices in Hospitals; Technology Development Program, Grant/Award Number: S3290500

## Abstract

**Objective:** The objective of the study was to evaluate the healing effect of hyaluronic acid films on palatal wounds.

**Materials and Methods:** After making 5-mm diameter palatal wounds, 72 rats were randomly assigned to three groups: control, hyaluronic acid gel, and hyaluronic acid film. The animals were sacrificed at 3, 7, and 21 days after the experiment. Clinical, histological, and RT-PCR analyses were performed. Human ex vivo oral mucosa models were used. Histological analysis and pan-cytokeratin staining were performed at 5 days after wound creation.

**Results:** In rat model, both gels and films showed favorable healing on Days 3 and 7 compared with healing in the control ( $p < 0.05$ ). Film showed remarkable VEGF and  $\alpha$ -SMA expression than did the others ( $p < 0.05$ ). Immunohistochemical analysis showed that film exhibited significantly lower CD68 and greater  $\alpha$ -SMA and vimentin expression levels than those in the others ( $p < 0.05$ ). In human model, re-epithelialization rate of film group was significantly higher than that of the others. Complete epithelial regeneration was confirmed only in film group using pan-cytokeratin staining.

**Conclusions:** Within the limits of this study, hyaluronic acid film outperformed gels in terms of palatal wound healing in both models.

## KEYWORDS

drug vehicle, gingiva, hyaluronic acid, wound healing

## 1 | INTRODUCTION

Free gingival graft (FGG) is the gold standard approach to repair mucogingival deformities and for periodontal soft tissue augmentation to increase the keratinized tissue volume in the dentoalveolar area

(Agarwal et al., 2015). It is effective in preventing gingival recession because it provides sufficient thickness and width of attached gingiva and improves the tissue biotype (Rateitschak et al., 1979; Wyrębek et al., 2018; Zucchelli et al., 2020). It also attenuates root hypersensitivity and reduces vestibular depth (Silva et al., 2010).

Although studies of FGG focus more on the recipient site, post-operative morbidity is closely related to the large uncomfortable donor site, followed by pain, bone exposure, bleeding, and infection (Wilhelm et al., 2017; Yussif et al., 2021). Palatal mucosa is a common donor site, as it has been shown high predictability and excellent healing outcomes (Miller & Allen, 1996). However, a previous clinical trial reported that using the palate as a donor site for FGG causes more pain than other periodontal surgical techniques, such as the single-incision and the trap-door method (Del Pizzo et al., 2002). Moreover, the wound healing is often delayed because the palatal donor site recovers tissue through secondary intention. This healing process requires the migration of epithelial cells from the periphery to the center (Hämmerle & Giannobile, 2014) and the removal of large amounts of connective tissue (Del Pizzo et al., 2002).

To overcome these issues, topical delivery of wound-healing materials has been proposed. In previous studies, topical delivery of hyaluronic acid (HA) gel exhibited improved palatal wound healing (Taskan et al., 2021; Yıldırım et al., 2018). These results are related to protecting the wound from oral bacterial contamination (Farsaei et al., 2012) and the biological properties of HA, such as angiogenesis, anti-inflammation, and antioxidant (Ke et al., 2013; Litwiniuk et al., 2016). HA positively affects gingival fibroblast proliferation and migration (Asparuhova et al., 2019) and accelerates tissue regeneration and healing. Moreover, HA can attract and retain moisture, resulting in reduced scar formation (Yıldırım et al., 2018).

However, the topical delivery of gel-based materials has some drawbacks because of their rapid degradation and weak adhesive properties (Simões et al., 2018). Topical delivery of HA gel can be limited in the oral environment because of saliva fluidity and dynamic changes in the oral environment. Therefore, we developed a film-type HA-based material with orodispersible properties and evaluated the healing effect of the HA film on palatal wounds. The null hypothesis was that wound healing at the donor site after FGG did not differ in the form HA was delivered, whether in a gel or film form.

## 2 | MATERIALS AND METHODS

### 2.1 | HA film preparation

Low molecular weight (0.8–1.2 MDa) HA films were prepared with a diameter of 7 mm according to previous studies (Kweon & Park, 2021; Lee, Lee, et al., 2022; Lee, Park, et al., 2022). The amount of HA was equivalent to 100 mL of 1% HA gel (Gengigel®; Ricerfarma). To confirm the consistency of sodium hyaluronate on both sides of the HA film, Fourier transform infrared spectroscopy (FTIR) spectra was measured using an FTIR spectrometer system (Nicolet5700; Thermo electron Co.) coupled to an attenuated total reflectance (ATR) mode (Figure 1). The FTIR-ATR spectra were analyzed at room temperature in the range 4000–400 cm<sup>-1</sup>.

### 2.2 | Tissue adhesion test

To assess tissue adhesion properties of HA film, lap shear strength was evaluated followed to ASTM F2255-05, the standard test procedure for strength properties of tissue adhesives (Kull et al., 2013). Porcine skin (Biozoa Biological Supply Co. Ltd.) was washed and shaved. Then, the skin was cut into 60×20 mm rectangles and placed on the 37°C heater. Next, excess moisture was removed from the skin using sterile gauzes. The HA films with 20×20 mm were applied to the skin. Then, 20 µL of sterilized water was sprayed on the film surface and other pieces of skin were superimposed on the film surface. They were left in drying incubator (37°C/50%) with adding a 200 g weight for 1, 2, and 3 min as holding time. The lap shear strengths of HA films were measured by the texture analyzer (QM100SN, QMESYS) at 10 mm min<sup>-1</sup> tracking speed. Also, laboratory shear strength of HA gel was evaluated as control. Each test was performed triplicate.

### 2.3 | In vivo animal model

This study used a randomized controlled experimental design. The protocol was approved by the local ethics committee (KHMC-IACUC-21-013) and followed the NIH Guidelines for the Care and Use of Laboratory Animals (National Research Council Committee for the Update of the Guide for the & Use of Laboratory, 2011). The sample size calculation was performed using G\*Power software (v. 3.1.9.7. Heinrich Heine University, Düsseldorf, Düsseldorf, Germany) with a significance level of 0.05, a statistical power of 90%, and an effect size of 0.97. Based on a previous study, the estimated sample size was calculated (Cho, Kim, et al., 2021; Cho, Lee, et al., 2021). A minimal size of six samples per group was required.

#### 2.3.1 | Study design

Seventy-two male Sprague–Dawley rats (9 weeks old, weighing 250–300 g) were used in this study. The animals were, first, divided into groups of control ( $n = 24$ ), HA gel ( $n = 24$ ), and HA film ( $n = 24$ ). Each group was then subdivided into 3-day sacrifice group ( $n = 10$ ), 7-day sacrifice group ( $n = 7$ ), and 21-day sacrifice group ( $n = 7$ ). In the 3-day sacrifice groups the specimens from seven animals went through histological analysis, while the remaining animals went through wound healing biomarker analysis.

#### 2.3.2 | Surgical protocol

The animals were anesthetized intraperitoneally with 30 mg/kg of Zoletil 50 (Virbac Lab). First, the oral cavity was disinfected with 2% chlorhexidine solution after administering 2% lidocaine with 1:80,000 epinephrine. Next, a palatal wound was formed with a 5-mm diameter disposable biopsy punch for a full-thickness flap. The materials were

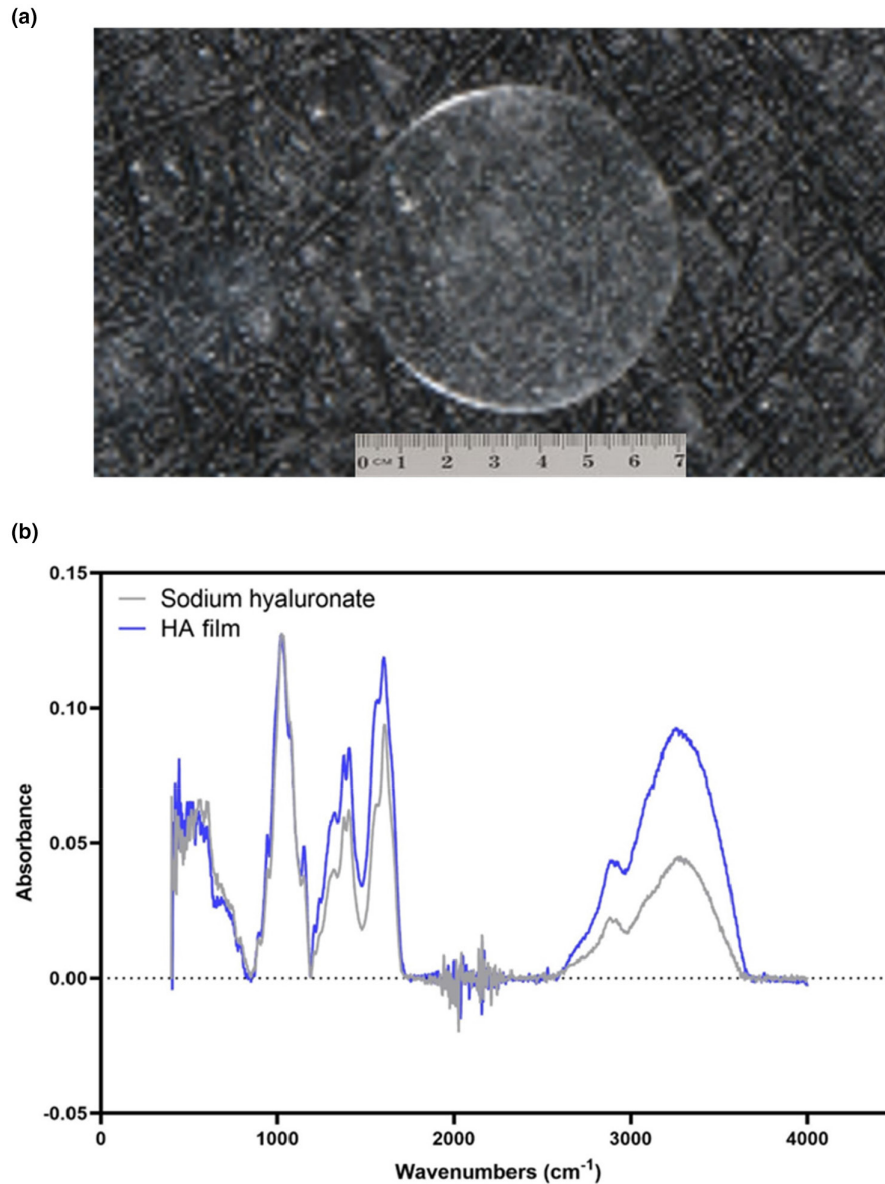


**FIGURE 1** Hyaluronic acid (HA) film. (a) HA film. (b) Fourier transform infrared spectroscopy (FT-IR) analysis. HA film shows similar bands with sodium hyaluronate.

applied after hemostasis. Then, the wound site was covered with gauze for 2 min. After the operation, the animals received intramuscular injection of penicillin G. After 3, 7, and 21 days, the animals were sacri-

of a 5-mm diameter circle was obtained using ImageJ software. Clinical wound healing (% unhealed area) was calculated as follows:

$$\text{Unhealed area (\%)} = (\text{pixel value of a 5 mm diameter circle} - \text{pixel value of the wound}) / (\text{pixel value of a 5 - mm diameter circle}) \times 100.$$

ficed under overdose of Zoletil 50 anesthesia (100mg/kg).

### 2.3.3 | Clinical wound healing analysis

Clinical wound healing was evaluated using a digital single-lens reflex camera and ImageJ software (National Institutes of Health). Images were obtained with each specimen placed on a 1-mm grid paper to compensate for the magnification and minimization. The pixel value

### 2.3.4 | Gene expression analysis by real-time polymerase chain reaction (RT-PCR)

The entire RNA was isolated from the 3-day sacrifice group ( $n = 3$  per group) and converted into complementary DNA using reverse transcriptase (SuperScript II Reverse Transcriptase; Invitrogen). Polymerase chain reaction (PCR) conditions were set up in 60°C annealing with 2× Power SYBR Green Master Mix (AB) reagent. RT-PCR was performed using the StepOnePlus RT-PCR system and

measured by SYBR green fluorescence using Power SYBR Green Master Mix (Thermo Fisher Scientific) within the following conditions: 15 min denaturation at 95°C, followed by 40 amplification cycles of denaturation for 15 s at 95°C, and annealing for 30 s at 59°C. Complementary DNA levels were normalized to glyceraldehyde-3-phosphate dehydrogenase (GAPDH) levels using the  $2^{-\Delta\Delta C_t}$  method. The primers in this study were as follows:

1. TNF- $\alpha$ , (F) 5'-CTGCCCAAGTACTTAGACATC-3', (R) 5'-AGAGC AATGACTCCAAAGTAG-3';
2. VEGF, (F) 5'-GGGCTCTGAAACCATGAACT-3', (R) 5'-CTTGG CATGGTGGAGGTACA-3';
3.  $\alpha$ SMA, (F) 5'-AGGGCTGTTTCCCATCCAT-3', (R) 5'-GCTGCCT TTTGGCCATT-3';
4. GAPDH, (F) 5'-ACAGTCAAGGCTGAGAATGG-3', (R) 5'-GATCT CGCTCTGGAAGATG-3'.

### 2.3.5 | Histological wound healing analysis

Extracted specimens were fixed in neutral buffered formalin (10%) and sectioned to a thickness of 2–3 mm suitable for tissue sampling. They were then placed into cassettes and introduced into the Myr Spin Tissue Processor STP120 automat (GRUPO MYR) for 13 h. Specimens were sliced to pass through the center of the wound along the coronal plane into 3- $\mu$ m sections using a microtome (RM2235; Leica). Slides were stained with Masson's trichrome and were observed with a slide scanner (Easyscanone, Motic). Histological wound healing was measured by evaluating the unhealed gap between the inner re-epithelial margins using the Motic DSAssistant 4 K (Motic) by two well-trained examiners.

Re-epithelialization (%) = (length of re-epithelialization of the left side + length of re-epithelialization of the right side) / (total wound length)  $\times$  100.

### 2.3.6 | Immunohistochemical analysis

For immunohistochemical (IHC) staining, specimens, including the palate, were fixed in neutral buffered formalin, embedded in paraffin, and sectioned at a thickness of 3 mm. The specimens were subjected to IHC staining using primary antibodies specific for CD68 (diluted 1:200; Ab125212, Abcam),  $\alpha$ -SMA (diluted 1:300; Ab7817, Abcam), and vimentin (diluted 1:500; Ab137321, Abcam). The sections were incubated overnight. After incubation, EnVision + System-HRP Labeled Polymer Anti-rabbit (K4003; Dako) was applied for 20 min. Color development was performed using a labeled DAB kit (3,3'-diaminobenzidine tetrachloride), and the samples were counterstained with Mayer's hematoxylin (Sigma-Aldrich). The specimens were scanned using a slide scanner (Easyscanone), and the area of the stained protein was calculated using ImageJ software by two well-trained examiners.

### 2.4 | Human oral mucosa equivalent ex vivo model

A 3D-reconstructed oral mucosa model (Neoderm®-OD, Seoul, Korea) in a 6-well plate form was used (Yang et al., 2018). The models were divided into same groups as rat model ( $n = 6$  per each group). A circular wound was formed onto the model by a 4-mm diameter biopsy punch. The maintenance medium was replaced per every 2 days, and the cells were incubated for 5 days at 37°C in humidified environment with 5% CO<sub>2</sub>. The model was then fixed in 4% paraformaldehyde, embedded in paraffin, and sliced after tissue processing. Each slide was stained with hematoxylin and eosin and analyzed using Image Pro (Media Cybernetics Inc.). Wound healing was analyzed according to re-epithelialization. The re-epithelialization percentage was calculated as follows:

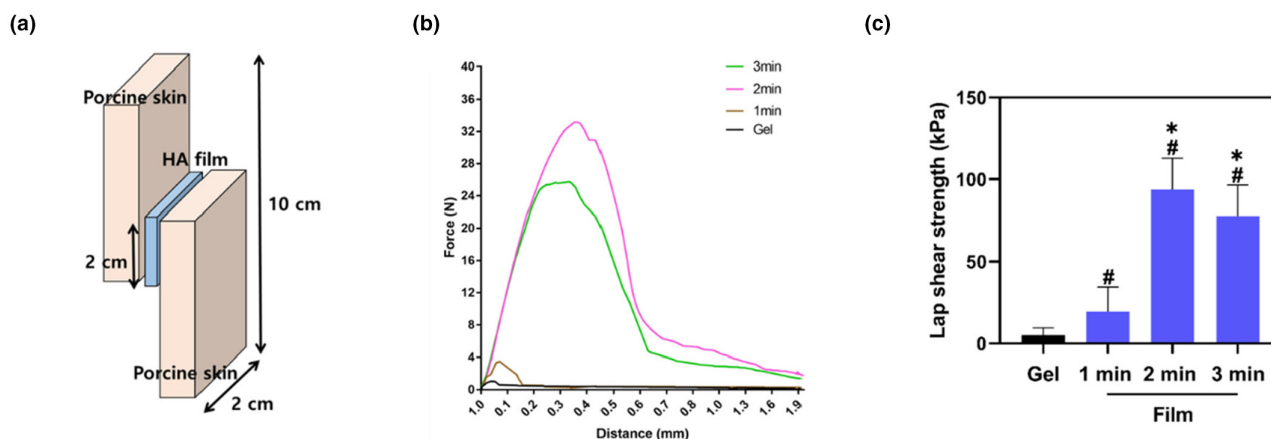


FIGURE 2 Tissue adhesion test. (a) Schematic design of tissue adhesion test, (b) maximum force curve of HA films according to gelation time, (c) lap shear strength. HA films showed higher strength values compared with that of gel. More than 2 min of gelation time showed significantly greater strength values ( $\#p < 0.05$  vs. gel,  $*p < 0.05$  vs. film with 1 min gelation).



Immunofluorescence staining with pan-cytokeratin was also performed. After paraffin block sectioning to a thickness of 5  $\mu\text{m}$ , the block was treated with citrate buffer for antigen retrieval and cleaned with PBS. The primary antibody, rabbit anti-human pan-cytokeratin, and the second antibody (anti-rabbit IgG FITC) were applied to the sections for 1 h, after which it was observed with a fluorescence microscope at a magnification of 100.

## 2.5 | Statistical analysis

The data were analyzed using IBM SPSS Statistics 20 (SPSS Inc.). To evaluate inter-observer reliability in IHC and histological analyses, the intraclass coefficient values (ICC) were calculated between the two examiners. With a score of 0.989 for histological analyses and 0.915 for IHC analyses, the ICC values were highly reliable. After the Kolmogorov–Smirnov test, the results were statistically evaluated by the Kruskal–Wallis test and the Mann–Whitney test ( $p < 0.05$ ).

## 3 | RESULTS

### 3.1 | Tissue adhesion test

Figure 2 shows maximum force curve of HA films according to gelation time. Gelation of HA film for  $>2$  min showed significantly higher lap shear strength ( $p < 0.05$ ).

### 3.2 | Clinical wound healing analysis

Regarding the unhealed area, significantly lower values in the HA gel and HA film groups compared with that in the control group were observed on Days 3 and 7 ( $p < 0.05$ ). However, there were no significant differences in the unhealed area between the two forms of HA

groups (Figure 3). On Day 21, clinical wound healing did not differ among the groups.

### 3.3 | RT-PCR

Figure 4 shows the expression levels of biomarkers associated with healing used in the comparison of the biological effects on early healing among the groups. The expression level of TNF- $\alpha$  was greater in both HA gel ( $p = 0.002$ ) and HA film ( $p = 0.002$ ) groups than that in the control group, and there were no significant differences between the two forms of HA groups. Regarding VEGF expression, the HA film group showed greater expression levels than the HA gel ( $p = 0.004$ ) and control ( $p = 0.015$ ) group. The HA film also showed greater  $\alpha$ -SMA expression than did the HA gel ( $p = 0.002$ ) and control groups ( $p = 0.041$ ). However, there were no significant differences in VEGF and  $\alpha$ -SMA expression between the HA gel and control groups.

### 3.4 | Histological healing analysis

The unhealed gap was lower in HA film group ( $2.77 \pm 0.21$  mm) compared with HA gel ( $4.10 \pm 0.24$  mm) and control groups ( $3.82 \pm 0.22$  mm) on Day 3 ( $p = 0.002$  and  $p = 0.004$ , respectively). However, no significant differences were observed between the HA gel and control groups. On Days 7 and 21, no differences in healing were observed among the three groups (Figure 5).

### 3.5 | IHC analysis

Figure 6 presents the results of the IHC analysis. The HA film group showed lower CD68 expression than the HA gel ( $p = 0.015$ ) and control groups ( $p = 0.01$ ). The expression levels of both  $\alpha$ -SMA and

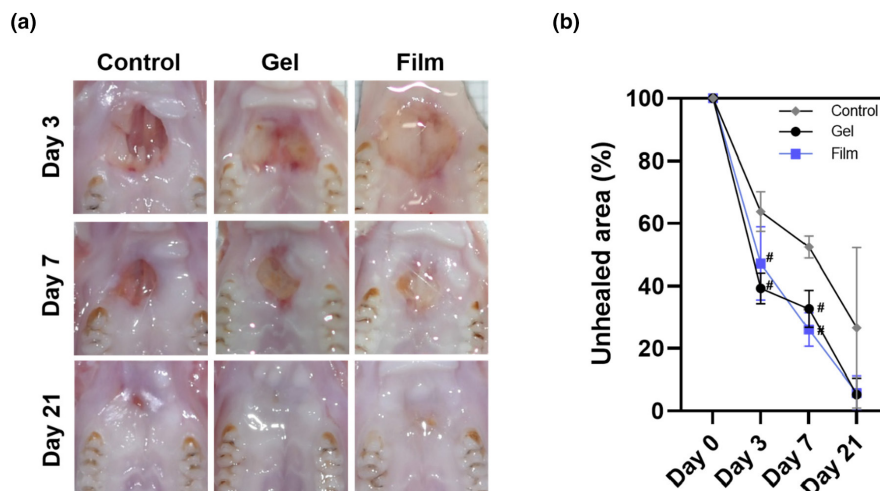


FIGURE 3 Clinical healing outcome. (a) Clinical photos of each group, (b) clinical healing outcome. The outcome was evaluated by calculating unhealed area (%). Both gel and film groups show more favorable healing during 7 days of healing. On Day 21, there were no significant differences in healing between the groups ( $\#p < 0.05$  vs. control).

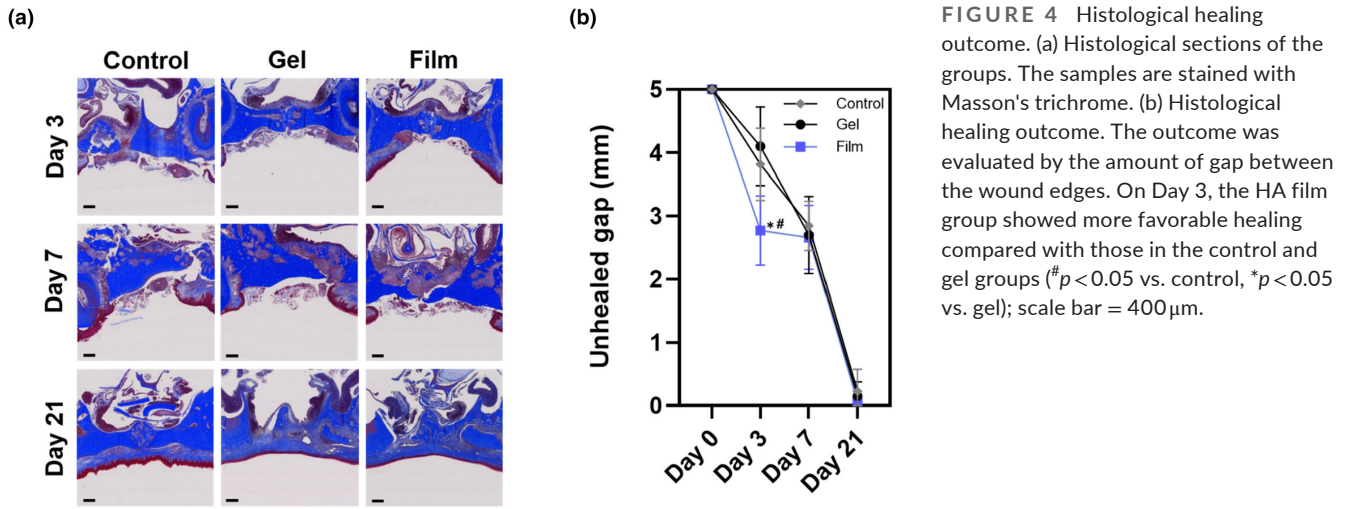


FIGURE 4 Histological healing outcome. (a) Histological sections of the groups. The samples are stained with Masson's trichrome. (b) Histological healing outcome. The outcome was evaluated by the amount of gap between the wound edges. On Day 3, the HA film group showed more favorable healing compared with those in the control and gel groups ( $\#p < 0.05$  vs. control,  $*p < 0.05$  vs. gel); scale bar =  $400\mu\text{m}$ .

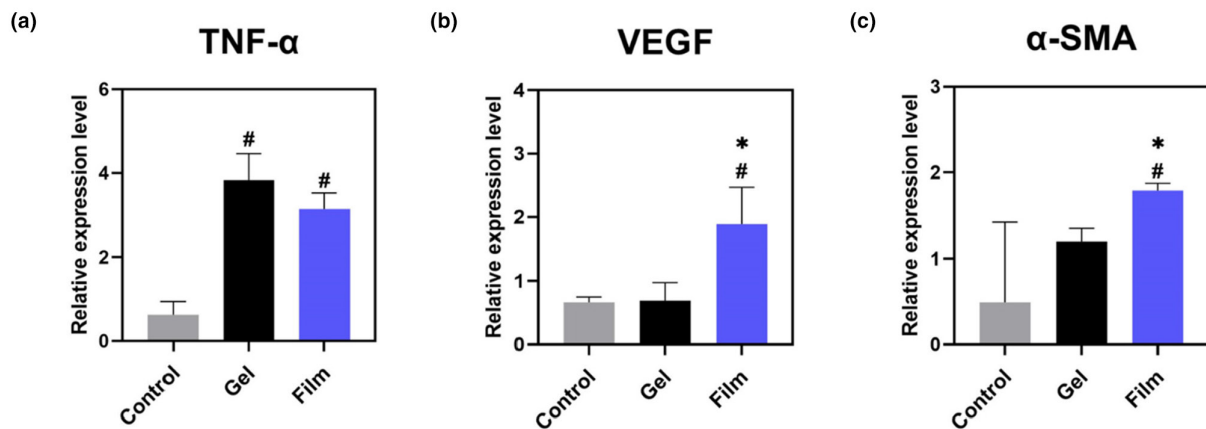


FIGURE 5 Expression of biomarkers on Day 3. (a) TNF- $\alpha$ , (b) VEGF, (c)  $\alpha$ -SMA ( $\#p < 0.05$  vs. control,  $*p < 0.05$  vs. gel). The data are expressed as mean  $\pm$  SD values of three independent experiments.

vimentin were greater in the HA film group than in the HA gel and control groups ( $p < 0.05$ ).

### 3.6 | Human oral mucosa equivalent ex vivo model

The re-epithelialization in the HA film group ( $98.37 \pm 1.63\%$ ) was higher than that of the HA gel ( $16.07 \pm 3.83\%$ ,  $p = 0.002$ ) and control groups ( $21.12 \pm 2.48\%$ ,  $p = 0.002$ ). No significant difference in the re-epithelialization rate was observed between the HA gel and the control groups. In the immunofluorescence images, complete epithelial regeneration was confirmed only in the HA film group (Figure 7).

## 4 | DISCUSSION

The present study evaluated the healing effects of HA films on palatal wound healing after FGG harvesting. The HA film promoted palatal wound healing, both clinically and histologically. The biological

markers related to oral soft tissue wound healing were also significantly upregulated in the HA film group.

The open palatal wound-like donor site of FGG heals approximately 2–4 weeks after surgery (Bosco & Bosco, 2007). The clinical healing outcomes of our study showed that both the HA gel and film groups showed accelerated wound healing over 7 days compared with the healing observed in the control group. The majority of the wound lesions healed after HA delivery on Day 21. This result is consistent with those of previous studies in which HA was applied on palatal donor sites after FGG harvesting (Yıldırım et al., 2018) or in post-extraction wound sites (Marin et al., 2020), which improved wound healing, especially in the early stages of healing. This effect may be related to the unique biological, physicochemical, and safety properties of HA (Fallacara et al., 2018; Marin et al., 2020).

Similar to the clinical healing outcomes, the HA film promoted wound healing histologically. The main histological outcome was that the HA film group showed a significant decrease in the unhealed gap compared with those in the HA gel and control groups on Day 3. Re-epithelialization is an important step in secondary

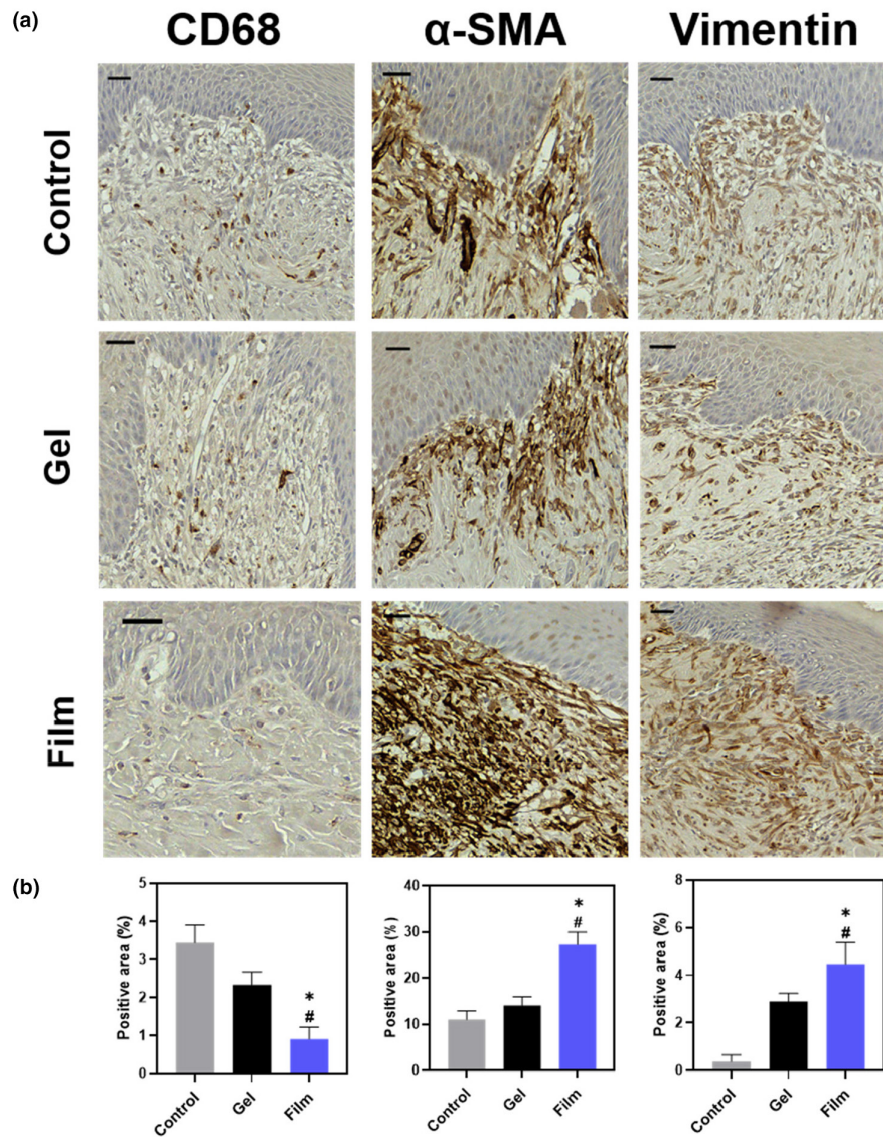


**FIGURE 6** Immunohistochemistry (IHC) analysis on Day 7. (a) Immunohistochemical-stained samples, (b) IHC-positive area (%) of CD68,  $\alpha$ -SMA, Vimentin (<sup>#</sup> $p < 0.05$  vs. control, \* $p < 0.05$  vs. gel); scale bar = 30  $\mu$ m.

wound healing (Pastar et al., 2014). During re-epithelialization, the epithelial cells move into the center of the lesion from the margin, cover the granulation tissue, and finally contact each other and stop migrating, thus completing the function (Santoro & Gaudino, 2005). Considering that the oral wound healing period is shorter than that of other organs (Cho, Kim, et al., 2021; Cho, Lee, et al., 2021), early re-epithelialization is a favorable clue for overall favorable healing.

Furthermore, to identify the differences and effectiveness in wound healing between HA film and HA gel, RT-PCR and IHC were performed. Inflammation, which accelerates vasodilation and induces cellular recruitment, is essential for successful regeneration and repair. TNF- $\alpha$ , a primary cytokine in the inflammation stage, was increased on Day 3 in both the HA gel and film groups. TNF- $\alpha$  stimulates the activation of keratinocytes, fibroblasts, and growth factors, and upregulates the antimicrobial defense system

(Piipponen et al., 2020). Chen and Abatangelo (1999) reported that higher concentrations of HA resulted in greater activation of TNF- $\alpha$  and also emphasized the role of HA. VEGF, a representative gene for angiogenesis, is important because it stimulates the degradation of the basement membrane, cell migration and proliferation (Bao et al., 2009), and regulation of extracellular matrix formation (ECM) (Keswani et al., 2013). Expression of VEGF was significantly higher in the HA film group on Day 3, which indicates that the HA delivery through the film was more stable and shortened the time from the early inflammatory stage to the later stage.

Induction of the inflammatory response in the early stages of wound healing is very important; conversely, it is crucial to inhibit the inflammatory response in the middle and late stages, respectively (Landén et al., 2016). IHC analysis performed on Day 7 confirmed that CD68, an indicator of macrophage and inflammatory response, was significantly reduced. At a certain time of healing, HA prevents

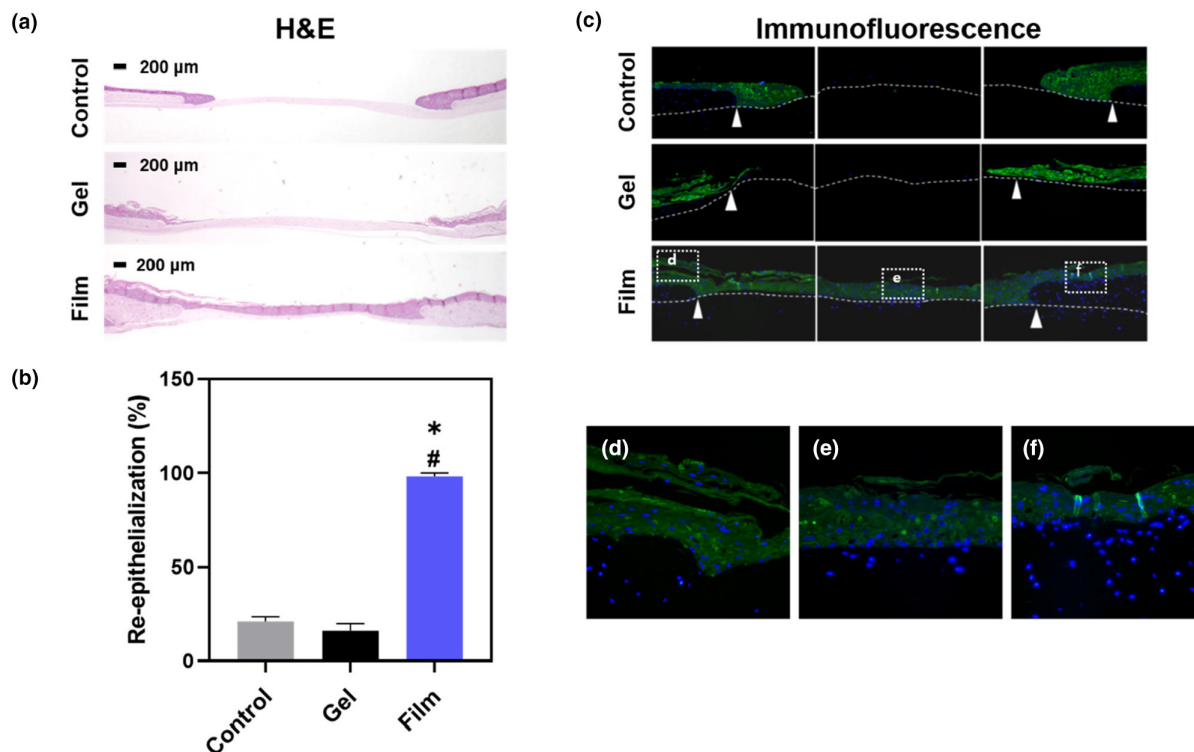


FIGURE 7 Human oral mucosa model. (a) Hematoxylin and eosin-stained samples, (b) re-epithelialization (%) (<sup>#</sup> $p < 0.05$  vs. control, <sup>\*</sup> $p < 0.05$  vs. gel) and (c) immunofluorescence images of the samples. The samples are stained with pan-cytokeratin. (d–f) High magnification of the corresponding square region in figure (c). Complete epithelial regeneration is observed in the newly healed area.

the migration of macrophages and neutrophils and helps dampening the inflammatory phase for proliferation and wound closure.

Following the late inflammatory phase, fibroblasts and myofibroblasts become key players in wound healing and remodeling. Fibroblast migration starts with the increase in levels of the cytokines and forms a framework, involving the ECM (including collagen) via myofibroblasts. Vimentin, a representative fibroblast marker, participates in numerous processes of wound healing, such as cell migration, fibroblast proliferation, cell adhesion, collagen accumulation, cytoskeletal arrangement, and signaling. The loss of vimentin leads to incomplete and prolonged wound healing (Cheng et al., 2016).  $\alpha$ -SMA is a molecular marker of myofibroblasts, a temporary but significant indicator of wound contraction and production of ECM, such as collagen, and it breaks down when the tissue is normalized. Vimentin levels significantly increased in the HA film on Day 7. Moreover,  $\alpha$ -SMA was expressed at higher levels on PCR Day 3 and confirmed by IHC on Day 7. Therefore, the HA film hastens the wound-healing cascade to form a structure.

In rats, differences in tissue composition and skin mobility and contraction are important healing process (Yao et al., 2014), whereas re-epithelialization is an important process in wound healing in humans. In an ex vivo human oral 3D model significantly superior re-epithelialization in the HA film group was observed. In the oral environment, where there is considerable movement and fluidity, gel-type formulations have limitations.

As previously revealed in vitro, the film form increases adhesion when it comes in contact with water; moreover, HA easily permeates into the tissues and facilitates the long-term expression of its unique functions and properties. The HA film facilitates high-quality regenerative wound healing, similar to the results of our ex vivo 3D experiment.

This study revealed facilitated proper palatal wound healing by applying HA in film type. Owing to their fast disintegration, dissolution, orodispersibility, and improved adhesive properties, HA films can overcome poor conditions of oral lesions such as infection, severe pH changes due to drinking or eating, and movements of the tongue (Walicová & Gajdziok, 2016). In addition, a film-type drug delivery system makes the application to the oral lesion easier and accurate; therefore, it is appropriate to utilize the unique function of HA in clinical practice. The comparison between HA gel and film in 3D human oral mucosa models (Lee et al., 2016), shown in this study, can also be used for further human-related studies.

However, the present study had some limitations. First, HA influences not only inflammation, proliferation, and ECM formation but also the remodeling phase, which is related to scar formation. Further studies conducted in the late remodeling phase are required. Second, although the action of the HA film could be indirectly estimated through indicators of the healing process, it is necessary to confirm the residual capacity of HA on the tissue to determine the need for reapplication of the HA film.

## 5 | CONCLUSIONS

In conclusion, HA film outperformed HA gels in terms of palatal wound healing in in vivo and ex vivo models, which suggests that HA film can be a promising therapeutic option for managing oral wound healing. Because film-type HA is easy for clinicians to apply and effective in the oral environment due to its adhesiveness, the orodispersible HA film is a viable option for promoting oral wound healing.

### ACKNOWLEDGEMENT

The authors thank Asiri Naif Mohammed for his time and contribution to the study.

### AUTHOR CONTRIBUTIONS

**Jeong Hyun Lee:** Data curation; formal analysis; writing – original draft. **Ko Eun Lee:** Validation; writing – original draft; writing – review and editing. **Sang Wook Kang:** Data curation; formal analysis. **Seung Hwan Park:** Data curation; formal analysis. **Yong Kwon Chae:** Writing – original draft. **Myoung-Han Lee:** Data curation; formal analysis; resources. **Dong-Keun Kweon:** Data curation; formal analysis; resources. **Sung Chul Choi:** Validation. **Ok Hyung Nam:** Conceptualization; data curation; validation; formal analysis; funding acquisition; writing – original draft; writing – review and editing.

### FUNDING INFORMATION

The authors are grateful for the support from Supporting Project to evaluation New Domestic Medical Devices in Hospitals, funded by the Ministry of Health and Welfare (MOHW) and the Korea Health Industry Development Institute (KHIDI). This work was supported by the National Research Foundation of Korea (NRF) grant funded by the Korea government (MSIT No. 2020R1C1C1006937) and supported by the Technology development program funded by the Ministry of SMEs and Startups (MSS, No. S3290500) and supported by Nano-Material Technology Development Program through the NRF funded by the Ministry of Science, ICT and Future Planning (No. K210307002).

### CONFLICT OF INTEREST STATEMENT

The authors report that there are no direct or indirect conflicts of interest involving associations with commercial entities that supported the work reported in the submitted manuscript, associations with commercial entities that might have an interest in the submitted manuscript, financial associations involving family members and other relevant non-financial associations.

### DATA AVAILABILITY STATEMENT

Datasets related to this article will be available upon request to the corresponding author.

### ETHICAL APPROVAL

Ethical approval was obtained from the Ethics in Institutional Animal Care and Use Committee of Kyung Hee Medical Center, Seoul, Korea (KHMC-IACUC-21-013).

### ORCID

Ko Eun Lee  <https://orcid.org/0000-0002-5641-4443>

Sang Wook Kang  <https://orcid.org/0000-0002-0358-2304>

Seung Hwan Park  <https://orcid.org/0000-0001-9298-3590>

Yong Kwon Chae  <https://orcid.org/0000-0001-8059-9305>

Sung Chul Choi  <https://orcid.org/0000-0001-7221-2000>

Ok Hyung Nam  <https://orcid.org/0000-0002-6386-803X>

### REFERENCES

- Agarwal, C., Tarun Kumar, A. B., & Mehta, D. S. (2015). Comparative evaluation of free gingival graft and AlloDerm® in enhancing the width of attached gingival: A clinical study. *Contemporary Clinical Dentistry*, 6(4), 483–488. <https://doi.org/10.4103/0976-237x.169838>
- Asparuhova, M. B., Kiryak, D., Eliezer, M., Mihov, D., & Sculean, A. (2019). Activity of two hyaluronan preparations on primary human oral fibroblasts. *Journal of Periodontal Research*, 54(1), 33–45. <https://doi.org/10.1111/jre.12602>
- Bao, P., Kodra, A., Tomic-Canic, M., Golinko, M. S., Ehrlich, H. P., & Brem, H. (2009). The role of vascular endothelial growth factor in wound healing. *The Journal of Surgical Research*, 153(2), 347–358. <https://doi.org/10.1016/j.jss.2008.04.023>
- Bosco, A. F., & Bosco, J. M. (2007). An alternative technique to the harvesting of a connective tissue graft from a thin palate: Enhanced wound healing. *The International Journal of Periodontics & Restorative Dentistry*, 27(2), 133–139.
- Chen, W. Y., & Abatangelo, G. (1999). Functions of hyaluronan in wound repair. *Wound Repair and Regeneration*, 7(2), 79–89. <https://doi.org/10.1046/j.1524-475x.1999.00079.x>
- Cheng, F., Shen, Y., Mohanasundaram, P., Lindström, M., Ivaska, J., Ny, T., & Eriksson, J. E. (2016). Vimentin coordinates fibroblast proliferation and keratinocyte differentiation in wound healing via TGF- $\beta$ -slug signaling. *Proceedings of the National Academy of Sciences of the United States of America*, 113(30), E4320–E4327. <https://doi.org/10.1073/pnas.1519197113>
- Cho, J. R., Lee, M. H., Oh, H. K., Kim, H., Kweon, D. K., Kang, S. M., Kim, B. K., Heo, C. Y., Kim, D. W., & Kang, S. B. (2021). Efficacy of hyaluronic acid film on perianal wound healing in a rat model. *Annals of Surgical Treatment and Research*, 101(4), 206–213. <https://doi.org/10.4174/ast.2021.101.4.206>
- Cho, Y. D., Kim, K. H., Lee, Y. M., Ku, Y., & Seol, Y. J. (2021). Periodontal wound healing and tissue regeneration: A narrative review. *Pharmaceuticals (Basel)*, 14(5), 456. <https://doi.org/10.3390/ph14050456>
- Del Pizzo, M., Modica, F., Bethaz, N., Priotto, P., & Romagnoli, R. (2002). The connective tissue graft: A comparative clinical evaluation of wound healing at the palatal donor site. A preliminary study. *Journal of Clinical Periodontology*, 29(9), 848–854. <https://doi.org/10.1034/j.1600-051x.2002.290910.x>
- Fallacara, A., Baldini, E., Manfredini, S., & Vertuani, S. (2018). Hyaluronic acid in the third millennium. *Polymers (Basel)*, 10(7), 701. <https://doi.org/10.3390/polym10070701>
- Farsaei, S., Khalili, H., & Farboud, E. S. (2012). Potential role of statins on wound healing: Review of the literature. *International Wound Journal*, 9(3), 238–247. <https://doi.org/10.1111/j.1742-481X.2011.00888.x>
- Hämmerle, C. H., & Giannobile, W. V. (2014). Biology of soft tissue wound healing and regeneration—consensus report of group 1 of the 10th European workshop on periodontology. *Journal of Clinical Periodontology*, 41(Suppl 15), S1–S5. <https://doi.org/10.1111/jcpe.12221>
- Ke, C., Wang, D., Sun, Y., Qiao, D., Ye, H., & Zeng, X. (2013). Immunostimulatory and antiangiogenic activities of low molecular weight hyaluronic acid. *Food and Chemical Toxicology*, 58, 401–407. <https://doi.org/10.1016/j.fct.2013.05.032>

- Keswani, S. G., Balaji, S., Le, L. D., Leung, A., Parvadia, J. K., Frischer, J., Yamano, S., Taichman, N., & Crombleholme, T. M. (2013). Role of salivary vascular endothelial growth factor (VEGF) in palatal mucosal wound healing. *Wound Repair and Regeneration*, 21(4), 554–562. <https://doi.org/10.1111/wrr.12065>
- Kull, S., Martinelli, I., Briganti, E., Losi, P., Spiller, D., Tonlorenzi, S., & Soldani, G. (2013). Glubran2 surgical glue: in vitro evaluation of adhesive and mechanical properties. *The Journal of Surgical Research*, 157(1), e15–e21. <https://doi.org/10.1016/j.jss.2009.01.034>
- Kweon, D. K., & Park, S. H. (2021). Method for manufacturing hyaluronate fibers by using melt spinning and hyaluronate fibers manufactured thereby. In: *Google Patents*.
- Landén, N. X., Li, D., & Stähle, M. (2016). Transition from inflammation to proliferation: A critical step during wound healing. *Cellular and Molecular Life Sciences*, 73(20), 3861–3885. <https://doi.org/10.1007/s00018-016-2268-0>
- Lee, J. H., Lee, K. E., Nam, O. H., Chae, Y. K., Lee, M. H., Kweon, D. K., Kim, M. S., Lee, H. S., & Choi, S. C. (2022). Orodispersible hyaluronic acid film delivery for oral wound healing in rats. *Journal of Dental Sciences*, 17, 1595–1603. <https://doi.org/10.1016/j.jds.2022.04.004>
- Lee, J. H., Park, S. H., Mohammed, A. N., Lee, M. H., Kweon, D. K., Chae, Y., Lee, K., Kim, M., Lee, H., Choi, S., & Nam, O. H. (2022). Effects of ginsenoside Rb1 loaded films on oral wound healing. *Journal Korean Acad Pediatr Dent*, 49(3), 300–309. <https://doi.org/10.5933/JKAPD.2022.49.3.300>
- Lee, O. J., Kim, J. H., Moon, B. M., Chao, J. R., Yoon, J., Ju, H. W., Lee, J. M., Park, H. J., Kim, D. W., Kim, S. J., & Park, H. S. (2016). Fabrication and characterization of hydrocolloid dressing with silk fibroin nanoparticles for wound healing. *Tissue Engineering and Regenerative Medicine*, 13, 218–226. <https://doi.org/10.1007/s1377-0-016-9058-5>
- Litwiniuk, M., Krejner, A., Speyrer, M. S., Gauto, A. R., & Grzela, T. (2016). Hyaluronic acid in inflammation and tissue regeneration. *Wounds*, 28(3), 78–88.
- Marin, S., Popovic-Pejcic, S., Radosevic-Caric, B., Trtić, N., Tatic, Z., & Selakovic, S. (2020). Hyaluronic acid treatment outcome on the post-extraction wound healing in patients with poorly controlled type 2 diabetes: A randomized controlled split-mouth study. *Medicina Oral, Patología Oral y Cirugía Bucal*, 25(2), e154–e160. <https://doi.org/10.4317/medoral.23061>
- Miller, P. D., Jr., & Allen, E. P. (1996). The development of periodontal plastic surgery. *Periodontology 2000*, 11, 7–17. <https://doi.org/10.1111/j.1600-0757.1996.tb00178.x>
- National Research Council Committee for the Update of the Guide for the Care and Use of Laboratory Animals. (2011). The national academies collection: Reports funded by National Institutes of Health. In *Guide for the care and use of laboratory animals*. National Academies Press (US).
- Pastar, I., Stojadinovic, O., Yin, N. C., Ramirez, H., Nusbaum, A. G., Sawaya, A., Patel, S. B., Khalid, L., Isseroff, R. R., & Tomic-Canic, M. (2014). Epithelialization in wound healing: A comprehensive review. *Adv Wound Care (New Rochelle)*, 3(7), 445–464. <https://doi.org/10.1089/wound.2013.0473>
- Piipponen, M., Li, D., & Landén, N. X. (2020). The immune functions of keratinocytes in skin wound healing. *International Journal of Molecular Sciences*, 21(22), 8790. <https://doi.org/10.3390/ijms21228790>
- Rateitschak, K. H., Egli, U., & Fringeli, G. (1979). Recession: A 4-year longitudinal study after free gingival grafts. *Journal of Clinical Periodontology*, 6(3), 158–164. <https://doi.org/10.1111/j.1600-051x.1979.tb02195.x>
- Santoro, M. M., & Gaudino, G. (2005). Cellular and molecular facets of keratinocyte reepithelialization during wound healing. *Experimental Cell Research*, 304(1), 274–286. <https://doi.org/10.1016/j.yexcr.2004.10.033>
- Silva, C. O., Ribeiro Edel, P., Sallum, A. W., & Tatakis, D. N. (2010). Free gingival grafts: Graft shrinkage and donor-site healing in smokers and non-smokers. *Journal of Periodontology*, 81(5), 692–701. <https://doi.org/10.1902/jop.2010.090381>
- Simões, D., Miguel, S. P., Ribeiro, M. P., Coutinho, P., Mendonça, A. G., & Correia, I. J. (2018). Recent advances on antimicrobial wound dressing: A review. *European Journal of Pharmaceutics and Biopharmaceutics*, 127, 130–141. <https://doi.org/10.1016/j.ejpb.2018.02.022>
- Taskan, M. M., Balci Yuce, H., Karatas, O., Gevrek, F., Isiker Kara, G., Celt, M., & Sirma Taskan, E. (2021). Hyaluronic acid with antioxidants improve wound healing in rats. *Biotechnic & Histochemistry*, 96(7), 536–545. <https://doi.org/10.1080/10520295.2020.1832255>
- Walicová, V., & Gajdziok, J. (2016). Oral films as perspective dosage form. *Ceská a Slovenská Farmacie*, 65(1), 15–21.
- Wilhelm, K. P., Wilhelm, D., & Bielfeldt, S. (2017). Models of wound healing: An emphasis on clinical studies. *Skin Research and Technology*, 23(1), 3–12. <https://doi.org/10.1111/srt.12317>
- Wyřębek, B., Górski, B., & Górska, R. (2018). Patient morbidity at the palatal donor site depending on gingival graft dimension. *Dental and Medical Problems*, 55(2), 153–159. <https://doi.org/10.17219/dmp/91406>
- Yang, K.-J., Son, J., Jung, S. Y., Yi, G., Yoo, J., Kim, D. K., & Koo, H. (2018). Optimized phospholipid-based nanoparticles for inner ear drug delivery and therapy. *Biomaterials*, 171, 133–143. <https://doi.org/10.1016/j.biomaterials.2018.04.038>
- Yao, Z., Huang, Y., Luo, G., Wu, J., & He, W. (2014). A biological membrane-based novel excisional wound-splinting model in mice (with video). *Burns Trauma*, 2(4), 196–200. <https://doi.org/10.4103/2321-3868.143625>
- Yıldırım, S., Özener, H., Doğan, B., & Kuru, B. (2018). Effect of topically applied hyaluronic acid on pain and palatal epithelial wound healing: An examiner-masked, randomized, controlled clinical trial. *Journal of Periodontology*, 89(1), 36–45. <https://doi.org/10.1902/jop.2017.170105>
- Yussif, N., Wagih, R., & Selim, K. (2021). Propylene mesh versus acrylic resin stent for palatal wound protection following free gingival graft harvesting: A short-term pilot randomized clinical trial. *BMC Oral Health*, 21(1), 208. <https://doi.org/10.1186/s12903-021-01541-z>
- Zucchelli, G., Tavelli, L., McGuire, M. K., Rasperini, G., Feinberg, S. E., Wang, H. L., & Giannobile, W. V. (2020). Autogenous soft tissue grafting for periodontal and peri-implant plastic surgical reconstruction. *Journal of Periodontology*, 91(1), 9–16. <https://doi.org/10.1002/jper.19-0350>

**How to cite this article:** Lee, J. H., Lee, K. E., Kang, S. W., Park, S. H., Chae, Y. K., Lee, M.-H., Kweon, D.-K., Choi, S. C., & Nam, O. H. (2023). Effect of orodispersible hyaluronic acid film on palatal mucosa wound healing. *Oral Diseases*, 00, 1–10. <https://doi.org/10.1111/odi.14517>